

Synthesis of CdS nanocomposites using macroporous ion-exchange resins

Mu-Li Wang, Chun-Hong Wang, Wei Wang*

*The Key Laboratory of Functional Polymer Materials of Ministry of Education and Institute of Polymer Chemistry,
College of Chemistry, Nankai University, Tianjin 300071, China*

Received 23 March 2006; received in revised form 16 January 2007; accepted 1 March 2007

Abstract

The preparation and characterization of nanocomposites composed of CdS nanocrystals in cross-linked polystyrene matrix were reported. The used matrix was commercial macroporous ion-exchange resins. Characterizations using transmission electron microscopy (TEM) and X-ray diffraction (XRD) show the nano-sized CdS crystals with an average size of about 9 nm. These nano-sized crystals can show the size-dependent UV–vis absorption and photoluminescence in comparison with bulk samples.

© 2007 Elsevier B.V. All rights reserved.

Keywords: Semiconductors; Precipitation; Luminescence

1. Introduction

During the past decades semiconductor nanoparticles have attracted much interest [1,2] because of the size-dependence of their functionalities, such as optical properties and photocatalytic activity as well as their promising applications in biological labeling and optical sensing, etc. [3]. Versatile chemical methods have been developed to synthesize high-quality semiconductor nanoparticles including sol–gel process [4], arrested precipitation in homogeneous solution [5], hydrothermal and solvothermal process [6] and synthesis in so-called nanoreactors such as micelles and vesicles and others [7].

CdS is one of the most important semiconductors that have been widely studied due to their interesting optical properties and photocatalytic activity. In practical applications CdS nanoparticles are needed to be incorporated into a stable host matrix to form composites [8–16]. Normally, there are two approaches to fabricate nano-sized CdS composites. One is to directly incorporate the preformed CdS nanoparticles into polymeric and inorganic matrix [8] or to polymerize monomer suspensions containing CdS nanoparticles [9]. Another approach is in situ synthesis of CdS nanoparticles from their precursors in confined spaces of some porous matrices via the ion-exchange route. Porous glass and aluminum [10], mesoporous silica [11], zeolite [12], carbon nanotube

[13], montmorillonite [14], layered metal oxides [15] have been employed.

In 1992, Ziolo et al. have used macroporous ion-exchange resins to prepare γ -Fe₂O₃/polymer nanocomposite with magnetic functionality [16]. The size of γ -Fe₂O₃ crystals are within 5–10 nm because the channel of porous resins not only provide spatially localized sites for nucleation but also minimize the degree of aggregation of the as-synthesized γ -Fe₂O₃ nanoparticles. This pioneer work has attracted great attention in the past two decades mainly because ion-exchange resins used are commercial available and the method is very facile. Herein, we report our synthesis of CdS nanoparticles inside the channel of macroporous ion-exchange resins via the route similar to that reported in Ref. [16]. The preparation process was simple because Cd²⁺ was introduced into the channel via ion-exchange to replace Na⁺ and then combined with S²⁻ to form CdS crystals in the channels of the resin. Our characterizations using transmission electron microscopy (TEM) and X-ray diffraction (XRD) demonstrate that the CdS crystals are nano-sized because of their formation in the confined condition. So, these nano-sized crystals can show the size-dependent functionalities, such as the blue shifts of the UV–vis absorption and photoluminescence in comparison with bulk samples.

2. Experimental

CdCl₂ and Na₂S were analytical reagent grade and were used without further purification. The resin used in this study was a macroporous cation-exchange resin manufactured by the Chemical Plant of NanKai University (PR China)

* Corresponding author. Tel.: +86 2223498126; fax: +86 2223498126.
E-mail address: weiwang@nankai.edu.cn (W. Wang).

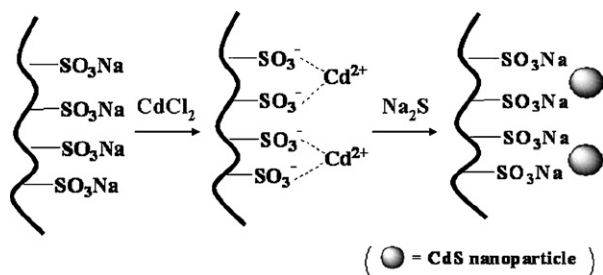


Fig. 1. Schematic of the CdS nanocrystal precipitation process using Cd^{2+} in an ion-exchange resin (D072).

with the marketed name D072 having a pore size in range of 10–100 nm. This ion-exchange resin is composed of sulfonated polystyrene, which is cross-linked with divinylbenzene to create a three-dimensional, porous polymer network. The functional group of the resin is sodium sulfonate and the dry resin has a nominal cation exchange capacity of 4.2 meq g^{-1} and was used in form of the spherical beads having diameters of 0.3–0.6 mm.

The synthesis process of D072/CdS nanocomposite is represented schematically as in Fig. 1. Typically, 2.0 g D072 was exchanged with Cd^{2+} from aqueous solution of CdCl_2 (40 mL, 0.2 M) under room temperature. After the resin was repeatedly washed with deionized water to remove excess physisorbed Cd^{2+} , S^{2-} was introduced by dropping Na_2S solution (60 mL, 0.2 M) and then the heterogeneous aqueous solution was refluxed for 24 h. This process produced 2.57 g yellow CdS/D072 composite. The loading content of CdS crystals in the composite is 22.2% by weight.

The powder X-ray diffraction (XRD) patterns were measured using a Rigaku D/Max-2500 X-ray diffractometer equipped with a $\text{Cu K}\alpha$ radiation ($\lambda = 0.15418 \text{ nm}$) source operated at 30 kV/15 mA. The transmission electron microscopy (TEM) and high-resolution transmission electron microscopy (HRTEM) images and selected area electron diffraction (SAED) patterns were recorded using a Tecnai-G²20 transmission electron microscope operated at an accelerating voltage of 200 kV. Diffuse-reflectance UV–vis spectra of the samples were recorded on a JASCO V-70 UV–vis-nearinfrared spectrophotometer with a resolution of 1 nm over a wavelength range from 300 to 800 nm. Photoluminescence (PL) spectra were obtained using a SPEX FL-210 spectrofluorometer equipped with a Xenon lamp of 150 W as an excitation light source. Thermogravimetric analysis (TGA) was conducted using a NETZSCH TG209 thermoanalyzer in 10 mL min^{-1} nitrogen flow rate and a heating rate of $10^\circ\text{C min}^{-1}$.

3. Results and discussion

Fig. 2 shows the XRD patterns of the ion-exchange resin D072 (dash line) and as-synthesized D072/CdS nanocomposite

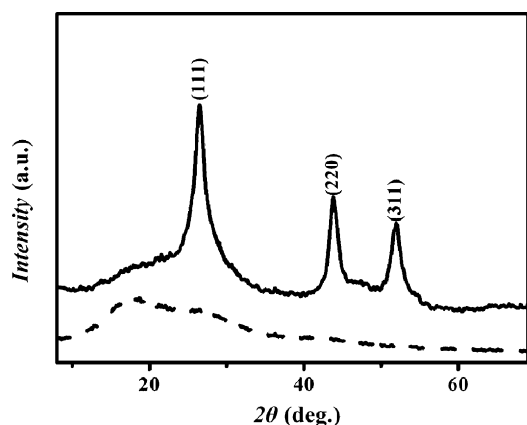


Fig. 2. XRD patterns of CdS nanocrystals in the composite (solid line) and the D072 (dash line) for comparison.

(solid line) in the 2θ range of $5\text{--}70^\circ$. For the composite three broadened peaks appear at $2\theta = 26.4^\circ$, 43.7° and 51.9° , respectively, corresponding to the (1 1 1), (2 2 0) and (3 1 1) lattice planes of CdS crystals. The appearance of these peaks further implies that the CdS crystals are in the pure cubic zinc-blend structure with a cell constant of $a = 0.583 \text{ nm}$, which was in agreement with the literature values (JCPDS Card, No. 10-0454). Based on the half-width of the (1 1 1) reflection the average size of CdS crystals calculated according to the Scherrer formula [17] was about 7 nm. Note a weak but broad hole around $2\theta = 20^\circ$ for the D072/CdS nanocomposite due to the presence of amorphous polystyrene matrix of the D072 resin.

Fig. 3A shows a TEM image of the CdS nanocrystals obtained from a typical D072/CdS nanocomposite. These nano-sized crystals have an irregular shape. The selected area electron diffraction (SAED) pattern in Fig. 3B exhibit the three sharp rings having the same Miller indexes as those obtained from XRD analysis, indicating again that CdS nanocrystals are in cubic crystalline phase. Fig. 3C is a histogram of the crystal sizes derived from the image in Fig. 3A and the others of the same sample (not shown). The average size of CdS crystals is about 9 nm. The solid curve is the fitting result obtained using a Gaussian function. A standard derivation of 14% indicates a relatively narrow-distribution. The TEM size of about 9 nm is larger than the XRD dimension of about 7 nm, but still within the error margins of both experiments. In addition CdS nanopar-

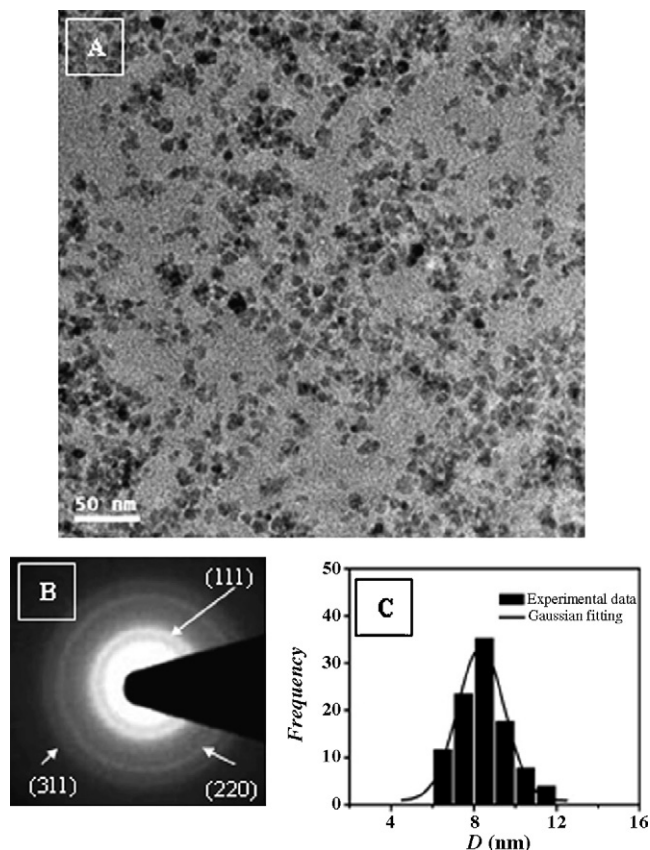


Fig. 3. (A) TEM image of the CdS nanocrystals, (B) SAED pattern of CdS nanocrystals and (C) CdS crystal size distribution.

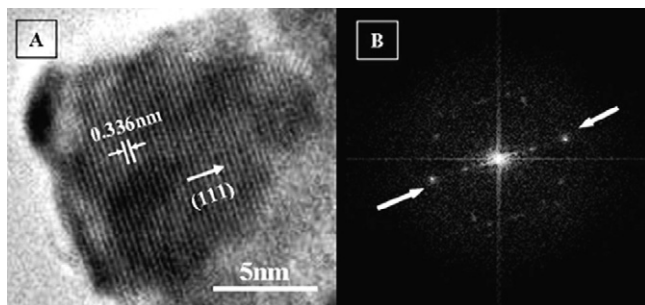


Fig. 4. (A) HRTEM image of a CdS nanocrystal showing the (111) plane and (B) corresponding FFT pattern.

particle size does not show a clear change after aging at ambient conditions for several months.

The results of XRD and TEM underscore the critical role played by the nano-sized channel within the ion-exchange resin in the formation of nano-sized CdS crystals. It is well known that precipitation of CdS in conventional conditions will produce particles with dimension in micrometer level due to aggregation. In the presence of the resin matrix, Cd^{2+} dispersed on the surface of channel of the matrix, and the nucleation and growth of CdS crystals happened immediately when S^{2-} diffused to the surface of channel to combine with Cd^{2+} . The nano-sized channel of the matrix confines the growth of CdS crystals and minimizes the degree of aggregation of the yielded nanocrystals. Consequently, the stable CdS nanoparticles dispersed well in the as-prepared nanocomposite.

The fine structure of the CdS nanocrystals of the cubic structure is further investigated by HRTEM. Fig. 4A provides a HRTEM image showing a CdS crystal in the composite, while Fig. 4B is the corresponding FFT pattern. The crystalline CdS shows the regular projection lines of the (111) lattice plane and the distance between the lattice planes is exactly 0.336 nm, which is consistent with the result of the XRD measurement.

Fig. 5 shows the UV–vis diffuse-reflectance spectra of the D072 (dot line), the D072/CdS nanocomposite (dash line) and the bulk CdS (dot-dash line) and the PL spectrum (solid line) of

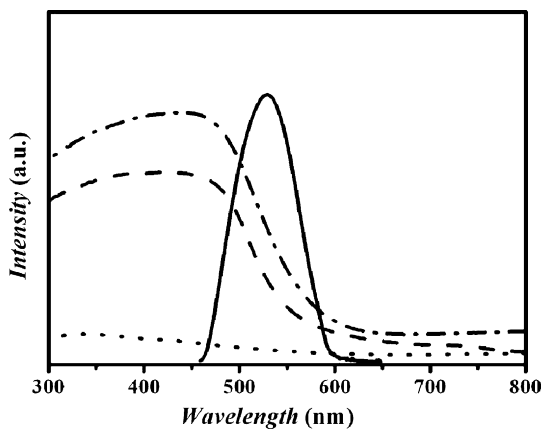


Fig. 5. Diffuse-reflectance UV–vis spectra of CdS nanocrystals/D072 composite (dash line), the D072 ion-exchange resin (dash-dot line) and bulk CdS (dot line) and PL spectra of CdS nanocrystals/D072 composite excited at 365 nm (solid line).

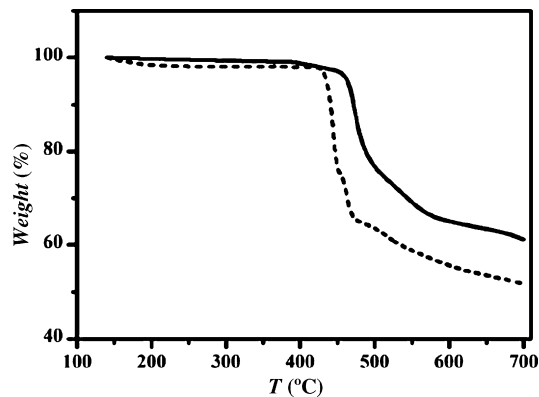


Fig. 6. TGA traces of a CdS nanocrystals/D072 composite (solid line) and the D072 ion-exchange resin (dash line).

the D072/CdS nanocomposite. The D072 resin does not show any absorption in the wavelength range of 300–800 nm, while the D072/CdS composite and bulk CdS show a broad absorption from 300 to 600 nm. The absorption edges are 505 nm for the D072/CdS composite and 520 nm for the bulk CdS determined by applying 2-order differentiation on the absorption spectrum. It is well known that CdS nanocrystallites with particle size below 6 nm should show strong quantum-size effect and the absorption edge should be blue-shifted with decreasing size [18]. D072/CdS nanocomposite prepared in this work shows a weak quantum size effect as the average size of CdS crystals is slightly larger than the critical size. When excited by $\lambda_{\text{ex}} = 365$ nm source, a broad PL peak centered at 525 nm is observed for the composite. This green emission is attributed to the near-band-edge emission of CdS crystals in the composite.

Fig. 6 shows TGA curves of D072 (dash line) and D072/CdS nanocomposite (solid line). The major weight-loss occurs above 420 °C for D072 and 480 °C for the CdS composite. The residual weight at 700 °C is 51 and 62% for D072 and CdS composite, respectively. Assuming that the difference of residual weight between these two samples are simply due to the presence of CdS and the decomposition of CdS below 700 °C can be neglected, the weight content of CdS in D072/CdS composite can be estimated to be 22.4% by the formula $W_{\text{CdS}} + (1 - W_{\text{CdS}}) \times 0.51 = 0.62$, where W_{CdS} refers to the weight content of CdS and $(1 - W_{\text{CdS}}) \times 0.51$ to the weight content of residual isolated ion-exchange resin at 700 °C. This value is similar to the loading content.

4. Conclusions

In summary, we have demonstrated a simple route to synthesize CdS nanocomposites using macroporous ion-exchange resins. In the nano-sized channel of ion-exchange resins Cd^{2+} ions exchange with Na^+ ions and then combine with S^{2-} to form the CdS nanoparticles. Our characterizations using XRD, TEM and TGA show that the average size of CdS crystals is 9 nm and the content is 22% by weight after only one loading. The D072/CdS composite is expected to be useful in some potential applications, for instance, as photocatalyst in solid phase

organic chemistry owing to the advantage of the thermal and solvent stability of D072.

Acknowledgements

We greatly appreciate Nankai University for a start-up funding to support this work. We also thank Prof. He-Xian Li for the PL measurement and Dr. Yan-Feng Ma for the UV–vis measurement.

References

- [1] C.B. Murry, C.R. Kagan, M.G. Bawendi, *Annu. Rev. Mater. Sci.* 30 (2000) 45.
- [2] K. Rajeshwar, N.R. de Tacconi, C.R. Chenthamarakshan, *Chem. Mater.* 13 (2001) 2765.
- [3] (a) M. Bruchez, M. Moronne, P. Gin, S. Weiss, A.P. Alivisatos, *Science* 281 (1998) 2013;
(b) W.C. Chan, S.M. Nie, *Science* 281 (1998) 2016;
(c) Y.K. Jaiswal, H. Mattoussi, J.M. Mauro, S.M. Simon, *Nat. Biotechnol.* 21 (2003) 47;
(d) X.F. Lu, Y.Y. Zhao, C. Wang, *Adv. Mater.* 17 (2005) 2485.
- [4] N.I. Kovtyukhova, E.V. Buzaneva, C.C. Waraksa, B.R. Martin, T.E. Mallouk, *Chem. Mater.* 12 (2000) 383.
- [5] C.C. Chen, C.Y. Chao, Z.H. Lang, *Chem. Mater.* 12 (2002) 1516.
- [6] (a) X. Dan, Z.P. Liu, J.B. Liang, Y.T. Qian, *J. Phys. Chem. B* 109 (2005) 14344;
(b) B. Liu, G.Q. Xu, L.M. Gan, C.H. Chew, *J. Appl. Phys.* 89 (2001) 1059.
- [7] (a) M.P. Pileni, *J. Phys. Chem.* 97 (1993) 6961;
(b) M.P. Pileni, *Langmuir* 13 (1997) 3266;
(c) B. Korgel, H.G. Monbouquette, *J. Phys. Chem.* 100 (1996) 346;
(d) W. Xu, D.L. Akins, *Mater. Lett.* 58 (2004) 2623.
- [8] (a) X.F. Lu, Y.Y. Zhao, C. Wang, Y. Wei, *Macromol. Rapid Commun.* 26 (2005) 1325;
(b) T. Hirai, T. Saito, I. Komasa, *J. Phys. Chem. B* 104 (2000) 11639;
(c) L. Pedone, E. Caponetti, M. Leone, V. Militello, V. Pantò, S. Polizzi, M.L. Saladino, *J. Colloid Interface Sci.* 284 (2005) 495;
(d) T. Hirai, Y. Bando, I. Komasa, *J. Phys. Chem. B* 106 (2002) 8967;
(e) C.-W. Wang, M.G. Moffitt, *Langmuir* 20 (2000) 11784;
(f) H. Zhang, Z. Zhou, K. Liu, R.B. Wang, B. Yang, *J. Mater. Chem.* 13 (2003) 1356.
- [9] (a) Y. Liu, E.C.Y. Liu, N. Pickett, P.J. Skabara, S.S. Cummins, S. Ryley, A.J. Sutherland, P. O'Brien, *J. Mater. Chem.* 15 (2005) 1238;
(b) J. Lee, V.C. Sundar, J.R. Heine, M.G. Bawendi, K.F. Jensen, *Adv. Mater.* 12 (2000) 1102.
- [10] (a) N.I. Kovtyukhova, B.K. Kelley, T.E. Mallouk, *J. Am. Chem. Soc.* 126 (2004) 12738;
(b) D. Routkevitch, T. Bigioni, M. Moskovits, J.M. Xu, *J. Phys. Chem.* 100 (1996) 14037.
- [11] (a) S.Z. Wang, D.G. Choi, S.M. Yang, *Adv. Mater.* 14 (2002) 1311;
(b) C. Tura, N. Coombs, Ö. Dag, *Chem. Mater.* 17 (2005) 573;
(c) Z.T. Zhang, S. Dai, X.D. Fan, D.A. Blom, S.J. Pennycook, Y. Wei, *J. Phys. Chem. B* 105 (2001) 6755.
- [12] N. Herron, Y. Wang, M.M. Eddy, G.D. Stucky, D.E. Cox, K. Moller, T. Bein, *J. Am. Chem. Soc.* 111 (1989) 530.
- [13] (a) J.M. Haremza, M.A. Hahn, T.D. Krauss, S. Chen, J. Calcines, *Nano Lett.* 2 (2002) 1253;
(b) S. Ravindran, S. Chaudhary, B. Colburn, M. Ozkan, C.S. Ozkan, *Nano Lett.* 3 (2003) 447.
- [14] Z. Han, H. Zhu, S.R. Bulcock, S.P. Ringer, *J. Phys. Chem. B* 109 (2005) 2673.
- [15] W.F. Shanguang, A. Yoshida, *J. Phys. Chem. B* 106 (2002) 12227.
- [16] R.F. Ziolo, E.P. Giannelis, B.A. Weinstein, M.P. O'Horo, B.N. Ganguly, V. Mehrotra, M.W. Russell, D.R. Huffman, *Science* 257 (1992) 219.
- [17] (a) P. Scherrer, *Nachrichten Gesellschafts Wissenschaftlich Göttingen* 2 (1918) 96;
(b) H.P. Klug, L.E. Alexander, *X-ray Diffraction Procedures*, John Wiley and Sons, New York, 1959.
- [18] (a) L.E. Brus, *J. Chem. Phys.* 80 (1984) 4464;
(b) A. Henglein, *Chem. Rev.* 89 (1989) 1861.